The Amplitude and Spectral Index of the Large Angular Scale Anisotropy in the Cosmic Microwave Background Radiation

KEN GANGA[1], LYMAN PAGE[2]

Joseph Henry Laboratories, Physics Department, Jadwin Hall, Princeton University, Princeton, NJ 08544–0708

EDWARD CHENG[3]

NASA/Goddard Space Flight Center, Code 685.0, Greenbelt, MD 20771

STEPHAN MEYER[4]

Room Acc F100, Enrico Fermi Institute, University of Chicago, 5640 South Ellis Ave., Chicago, IL 60637

Received ______________________; accepted ______________________

[1]E-Mail: ganga@pupgg.princeton.edu

[2]E-Mail: page@pupgg.princeton.edu

[3]E-Mail: ec@stars.gsfc.nasa.gov

[4]E-Mail: meyer@oddjob.uchicago.edu

ABSTRACT

In many cosmological models, the large angular scale anisotropy in the cosmic microwave background is parameterized by a spectral index, n, and a quadrupolar amplitude, Q. For a Peebles-Harrison-Zel'dovich spectrum, $n = 1$. Using data from the Far Infra-Red Survey (FIRS) and a new statistical measure, a contour plot of the likelihood for cosmological models for which $-1 < n < 3$ and $0 \leq Q \leq 50$ μK is obtained. Depending upon the details of the analysis, the maximum likelihood occurs at n between 0.8 and 1.4 and Q between 18 μK and 21 μK. Regardless of Q, the likelihood is always less than half its maximum for $n < -0.4$ and for $n > 2.2$, as it is for $Q < 8$ μK and $Q > 44$ μK.

Subject headings: cosmology: cosmic microwave background

1. Introduction

With the *COBE*/DMR detection of anisotropy in the cosmic microwave background radiation (CMB) (Bennett et al. 1992; Smoot et al. 1992; Wright et al. 1992), followed by the FIRS–*COBE*/DMR cross-correlation (Ganga et al. 1993) and a host of recently reported detections on smaller angular scales, we must now characterize the nature of the detected variations.

The inflation model predicts a spectrum of primordial density perturbations of form $P(k) \propto k$ for large angular scales (Steinhardt & Turner 1984), while popular variants of cold dark matter (CDM) models predict $P(k) \propto k^n$ with $0.7 < n < 1$ (see Turner (1993) for a review). Textures will also appear scale-invariant (i.e., $n = 1$; Pen et al. 1994), while cosmic strings may mimic an n of 1.35–1.5 (Perivolaropoulos 1993). Thus, by limiting the range of n allowed by the data we can constrain theories of structure formation. It should be pointed out, however, that many theories are not well parameterized this way (*e.g.*, Ratra & Peebles (1994)) and that in this work we consider models with *Gaussian* fluctuations only.

If one assumes this power law spectrum for density perturbations in an Einstein-DeSitter universe, then the angular power spectrum of anisotropies in the CMB is given by (Bond & Efstathiou 1987)

$$C_l = Q^2 \frac{4\pi}{5} \frac{\Gamma\Big((2l+n-1)/2\Big)\Gamma\Big((9-n)/2\Big)}{\Gamma\Big((2l+5-n)/2\Big)\Gamma\Big((3+n)/2\Big)}, \tag{1}$$

where $Q = \sqrt{5C_2/4\pi}$ is a parameter that sets the amplitude of the theoretical angular power spectrum and correlation function at the angular scale of the quadrupole.[5] Note also that Equation 1 does not account for microphysical processes that can change the

[5]Smoot et al. (1992) use the notation Q_{rms-PS} to denote the parameter, but for the sake of brevity we follow the notation of Wright et al. (1994b) and use Q. Note that Q is *not*

power spectrum of anisotropies and thus alter the effective n; for example, "standard" scale invariant CDM has an effective n of 1.15 for $l \lesssim 30$ (Bond 1994).

The first estimate of n using large scale CMB anisotropy data was made by fitting the theoretical auto-correlation function (ACF) derived from Equation 1 directly to the auto-correlation function of the *COBE*/DMR first year data. The result was $n = 1.15^{+0.45}_{-0.65}$ and $Q = 16.3 \pm 4.6$ μK (Smoot et al. 1992). Seljak and Bertschinger (1993), using a maximum-likelihood analysis again on the first-year *COBE*/DMR data, found that $Q = (15.7 \pm 2.6)e^{0.46(1-n)}$ μK. Additionally, Smoot et al. (1994) and Torres (1994) have both done topological analyses of these data to limit n to $1.7^{+0.3}_{-0.6}$ and 1.2 ± 0.3, respectively. Bond (1994) has extracted the index from an analysis of the power spectrum of both FIRS and DMR. He finds $n = 1.8^{+0.6}_{-0.8}$ for FIRS and $n = 2.0^{+0.4}_{-0.4}$ for the first-year DMR maps. Wright et al. (1994b), using a power spectrum analysis with the two-year DMR maps, find $n = 1.46^{+0.41}_{-0.44}$. Bennett et al. (1994), also using the DMR two-year maps, perform a maximum-likelihood analysis with Monte Carlo simulations and find $n = 1.59^{+0.49}_{-0.55}$. Finally, Górski et al. (1994) use a power spectrum based method to compute the likelihood of models. Applying it to the DMR two-year data, they obtain a maximum likelihood at $(n, Q) = (1.2, 17\ \mu\mathrm{K})$ and a maximum in the marginal likelihood for n at 1.1 ± 0.3.

This range of results, often with the same data, indicates the need for more data and consistent statistical techniques. In this *Letter*, we describe a method for analyzing CMB anisotropy maps and apply it to the Far Infra-Red Survey (FIRS). This method uses the correlation function of anisotropy maps. Thus, it is relatively insensitive to noise sources that can plague analyses based upon the χ^2 or the power spectrum of a map (Bond 1994) and should provide a useful complement other methods.

---

the root-mean-squared amplitude of the quadrupole in our Universe; we do not measure the intrinsic quadrupole because of our limited sky coverage.

FIRS is a balloon-borne, bolometric anisotropy experiment that observes in four channels at 170, 290, 500 and 680 GHz. It has a beam full-width-at-half-maximum (FWHM) of 3.°8 and has been flown successfully twice, resulting in coverage over most of the Northern hemisphere. The data used here are from the 170 GHz channel of the October, 1989 flight and cover roughly one quarter of the sky. The experiment, map and processing are described more fully in Ganga et al. (1993), Meyer et al. (1991) and Page et al. (1989, 1990, 1992, 1994a,b). The map is a essentially a set of pixels i, each with an associated residual temperature t_i and statistical weight w_i. A 15° Galactic latitude cut has been imposed on these data and on the simulations described below to minimize the effects of residual dust emission near the Galactic plane. For this analysis, we assume that all the correlations in the map are due to correlations in the CMB. In Page et al. (1994b), the data reduction and known systematic errors are discussed. There are no *known* systematic effects that introduce correlations into the data at levels which affect the results of this analysis.

2. Analysis

The correlation function of the CMB is estimated from the data with

$$C(\theta_A) = \frac{1}{\Gamma_A} \sum_{i,j \in A} w_i w_j t_i t_j, \tag{2}$$

where the sum is over all pixels i and j for which the angle between them is θ_A and where $\Gamma_A = \sum_{i,j \in A} w_i w_j$. $C(\theta_A)$ is presented in Figure 1. Note that if the maps contain nothing but statistical noise, Γ_A is the reciprocal of the variance in bin A. That is, $\sigma^2_{C(\theta_A)} = 1/\Gamma_A$ (see Ganga et al. (1993) for a derivation and Smoot et al. (1994) for a discussion of weighting schemes for different statistics over CMB maps).

Simulations of the sky are made for each n from 0.9 to 2.9 in steps of 0.1 following the methods of Cottingham (1987) and Boughn et al. (1993). Specifically, maps of unit amplitude are made with underlying temperatures at each pixel i defined by

$$t_i = \sum_{l=2}^{l_{max}} \sum_{m=-l}^{l} a_{l,m} \sqrt{W_l} Y_{l,m}(\theta_i, \phi_i), \tag{3}$$

where W_l is related to the Legendre transform of the experiment's beam response. If one assumes that the response is Gaussian, as we do here (but see Wright et al. (1994a)), this window function can be approximated by $W_l = e^{-0.18 \cdot l(l+1)\theta_{1/2}^2}$, where $\theta_{1/2}$ is the FWHM of the beam (in radians). With a FWHM of 3.°8, W_l falls to 0.5 at $l = 29$. For these simulations, l_{max} is either 150 or the highest l for which $W_l C_l / W_2 C_2 > 10^{-7}$, whichever is lowest. Each $a_{l,0}$ is drawn from a normal distribution with a variance of $C_l/(0.8\pi Q^2)$ and for $m > 0$ both the real and imaginary parts of $a_{l,m}$ are drawn from normal distributions with variances of $C_l/(1.6\pi Q^2)$. Finally, $a_{l,-m} = (-1)^m a_{l,m}^*$. We call these signal maps. In order to include experimental uncertainties, separate noise maps are created. The temperature at each pixel i is drawn from a normal distribution with a variance of $1/w_i$. The pixels in both the signal and noise maps have the same weights as the real data. In order to match the processing done on the real data, an offset and a dipole are removed from each map separately in a least-squares fit.

With this prescription, we form $C_{SS}(\theta)$, the ACF of a signal map, $C_{SN}(\theta)$, the cross-correlation between a signal map and its associated noise map, and $C_{NN}(\theta)$, the ACF of a noise map. We note that the full ACF of a single sky realization with a particular value of Q and noise will be

$$C(\theta) = Q^2 \frac{4\pi}{5} C_{SS}(\theta) + 2Q\sqrt{\frac{4\pi}{5}} C_{SN}(\theta) + C_{NN}(\theta). \tag{4}$$

This scaling allows one to reduce the number of simulations made, though a set of simulations at each value of n to be tested is still required.

For each simulation we make the statistic

$$R = \sqrt{\frac{1}{\sum_A \Gamma_A} \sum_A \Gamma_A \Big(C_F(\theta_A) - C_D(\theta_A)\Big)^2}, \tag{5}$$

where $C_F(\theta_A)$ is the value of the ACF of a simulation at bin A and $C_D(\theta_A)$ is the value of the ACF of the data at correlation bin A. If $R = 0$, the ACF of the simulation is the same as that of the data.

We calculate the likelihood, $P(D|n, Q)$, or the relative probability of obtaining the FIRS data ACF given a model parametrized by n and Q, by choosing a limiting value, R_{lim}, for R and finding the number of simulations, N, for which $R < R_{lim}$. We normalize the distribution so that the maximum likelihood is unity. The *a posteriori* probability that the Universe is parameterized by a certain n and Q can then be found by invoking Bayes's theorem with a suitable *a priori* probability distribution for (n, Q) (see, for example, Martin (1971)).

In essence, we are treating the correlation functions as vectors in an n_c dimensional ACF space. The various R's represent the weighted magnitude of the difference between the data ACF vector and a simulation ACF vector. If the Γ_A's were all the same, R_{lim} would define the radius of an n_c dimensional sphere centered upon the data ACF. When the Γ_A are different, the sphere is deformed into an ellipsoid. By counting the number of simulations with R less than some chosen R_{lim}, we are calculating the density of simulated ACF's in the neighborhood of the measured ACF. This density is proportional to the likelihood. The method accounts for non-uniform sky coverage, instrumental noise, cosmic variance and the effects of removing an offset and dipole from the data.

3. Results and Discussion

Figure 2 shows the results of the analysis for $-1 < n < 3$ and $0\ \mu\mathrm{K} < Q < 50\ \mu\mathrm{K}$. In this case, $R_{lim} = 430\ (\mu\mathrm{K})^2$, resulting in $N_{max} = 171$ simulations at the most likely combination of (n, Q) with $R \leq R_{lim}$. That is, for $(n, Q) = (1.0, 19\ \mu\mathrm{K})$, 171 out of a total of 20000 simulations had R less than $430\ (\mu\mathrm{K})^2$. All other combinations of (n, Q) had fewer simulations fall within the test volume. Figure 2 shows likelihood contours for 0.05, 0.25, 0.5 and 0.75 with solid lines along with a large $\times$ at the maximum.

For each model, the number of simulations within our limiting radius is governed by the binomial distribution. The probability of a particular simulation falling within the test volume is much smaller than that of it falling outside the volume. We can, therefore, approximate the variance in the estimate of the various N's by N itself. Hence, the uncertainty in the probability for those models with $P(Q,n|D) \approx 1$ is approximately $\sqrt{2/N_{max}}$, and the error in the estimates of the likelihoods near the maximum likelihood in Figure 2 is approximately 11% (with $N_{\rm max} = 171$). Because there is a high ridge in the likelihood near the maximum, this is not a good method of finding the absolute maximum in the likelihood. Depending upon how R_{lim} is chosen, the maximum falls between $n = 0.8$ and $n = 1.4$. This is borne out by Figure 3, which shows that the (n,Q) with the maximum likelihood depends slightly on the values of R_{lim}, although not by amounts in excess of what is expected statistically.

Bond (1994) has noted that the these data contain "white noise." This is an excess variance in the FIRS data which may cause problems for analyses based on the power spectrum, such as those done by Bond and Gorski (1994). The work presented here side-steps this problem since, in principle, this noise affects only the $\theta_A = 0$ bin of the correlation function, which is not included in this analysis. To check the possibility that the noise has 'leaked' out of the zero ACF bin, the analysis was repeated after excising the bin at $\theta_A = 1.^\circ 4$ (effectively eliminating all correlations on angular scales less than $2.^\circ 8$). The results are consistent with those quoted above. If the data contained only white noise, Figure 2 would have a maximum near n = 3. Clearly, the white noise does not significantly effect these results. Again, this is because this method is primarily sensitive to spatial correlations in the data.

This method has been checked in a number of ways. Figure 3 shows that there are small changes in the likelihood contours as R_{lim} is increased. This indicates that a smaller value of R_{lim} is desirable. With this number of simulations, however, reducing R_{lim} degrades the plot to the point where it is no longer useful. Note though that the likelihood is stable for $n \approx 1$ and that for other n's the likelihood values are conservative (that is, the likelihood is *overestimated*).

We have also checked that changing the weighting in the definition of R does not affect the results. Redefining R such that

$$R = \sqrt{\frac{1}{\sum_A W_A} \sum_A W_A \Big(C_S(\theta_A) - C_D(\theta_A)\Big)^2}, \tag{6}$$

where W_A is now defined as Γ^m for various m yields consistent results. Specifically, for $m = 3/4$, $3/2$ and 2, the bounds on n are $-0.4 < n < 2.4$, $-0.8 < n < 2.0$ and $-0.8 < n < 2.0$ respectively. The small m dependence of the likelihood will be discussed in depth elsewhere, as will more exact estimation of the maximum likelihood (Ganga 1994).

We put limits on the bias of this method by applying the procedure to 500 additional simulations with $(n, Q) = (1.0, 20\ \ \mu\mathrm{K})$. Though not a well defined quantity because some of the simulations would naturally prefer an $n < -0.9$ or an $n > 2.9$, the mean result, $(n, Q) = (0.8, 16.5\ \ \mu\mathrm{K})$, is consistent with the input values to within the uncertainties in estimating the mean.

Figure 2 implies that for the FIRS data $n \approx 1$ is favored. We point out, however, that only a fraction of the total ACF space has been tested. Many other possibilities exist. Wright et al. (1992) found the ACF of the *COBE*/DMR first-year data to be well described by a Gaussian with a coherence angle, θ_c, of 13.°5; that is, the correlation function of the DMR data was fit well by a function of form $C(\theta) = C(0)e^{-0.5(\theta/\theta_c)^2}$ with adjustments for offset and dipole removal, where $C(0)$ is the variance of the intrinsic sky fluctuation. This statistical method is well suited to testing this possibility. Retaining the normalization used in Figure 2, we find the likelihood of such a model with $C(0) \approx (44 \;\; \mu\mathrm{K})^2$ to be 1.4. That is, 40% more likely than the most likely model based on a power law spectrum. Thus, while $n \approx 1$ may be the preferred power law model, we cannot prove it is the best model.

We emphasize that no one experiment can prove that the correlated signal measured is due solely to the CMB. However, in the case of the FIRS data we have ruled out correlation stemming from astrophysical foregrounds, the instrument, and analysis artifacts (Page et al. 1994b). The similarity of this result to the COBE/DMR auto-correlation function and the significant cross-correlation (Ganga et al. 1993) with DMR strongly suggest that both experiments are detecting correlations in the CMB. Work is underway to generalize our method to find the most likely (n, Q) for the FIRS/DMR cross-correlation.

4. Acknowledgements

We would like to thank Steve Boughn and Dick Bond for insights and suggestions. We also thank E. Bertschinger, F. Camilo, D. Cottingham, K. Górski, G. Hinshaw, B. Ratra, and N. Turok for helpful conversations, and the referree, L. Perivolaropoulos, for a swift report which improved this *letter*. This work was supported under NASA grants NAGW–1841 and NAG5–2412, NSF grant PH 89–21378, and an NSF NYI grant to L. Page.

REFERENCES

Bennett, C.L. et al. 1992, ApJ, 396(1):L7–L12

Bennett, C.L. et al. 1994, submitted to ApJ

Bond, J.R. 1994, In *Proceedings of the 1994 Capri CMBR Conference*

Bond, J.R. & Efstathiou, G. 1987, MNRAS, 226:665

Boughn, S.P. et al. 1993, ApJ, 391(2):L49–L52

Cottingham, D. 1987, PhD thesis, Princeton University

Ganga, K. 1994, PhD thesis, Princeton University

Ganga, K. et al. 1993, ApJ, 410:L57

Górski, K. et al. 1994, submitted to ApJ

Martin, B.R. 1971, *Statistics for Physicists*, Academic Press

Meyer, S.S., Cheng, E.S. & Page, L.A. 1991, ApJ, 371(1):L7–L9

Page, L.A. 1989, PhD thesis, Massachusetts Institute of Technology

Page, L.A. et al. 1994a, *Applied Optics*, 33(1):11–23

Page, L.A. et al. 1994b, In *Astrophysical Letters and Communications: Proceedings from the 1994 Capri CMBR Workshop*

Page, L.A., Cheng, E.S. & Meyer, S.S. 1990 ApJ, 355(1):L1–L4

Page, L.A., Cheng, E.S. & Meyer, S.S. 1992 *Applied Optics*, 31(1):95–100

Pen, U., Spergel, D. & Turok, N. 1994, *Phys. Rev. D*, 49, 2

Perivolaropoulos, L. 1993, Center for Astrophysics preprint CfA–3796

Ratra, B. & Peebles P.J.E. 1994, Princeton University Physics preprint PUPT-1444; Submitted to *Phys. Rev. D*

Seljak, U. & Bertschinger, E. 1993, ApJ, 417(1):L9–L12

Smoot, G.F. et al 1992, ApJ, 396(1):L1–L5

Smoot, G.F. et al. 1994, submitted to ApJ

Steinhardt P.J. & Turner, M.S. 1984, *Physical Review D*, 29:2162

Torres, S. 1994, ApJ, 423(1):L9–L12

Turner, M.S. 1993, FERMILAB-Conf-92/313-A

Wright, E.L. et al. 1992, ApJ, 396(1):L13–L18

Wright, E.L. et al. 1994a, ApJ, in press

Wright, E.L. et al. 1994b, submitted to ApJ

This manuscript was prepared with the AAS LaTeX macros v3.0.

5. Figure Captions

Fig. 1. — The FIRS auto-correlation function. The error bars represent the variations due to experimental noise only. For this plot, the 180° span of θ_A is divided into 40 bins each of width 4.°5. Due to the limited sky coverage, only 36 bins contain data. The shaded area shows the 1σ spread in the 20000 simulated auto-correlation functions for $n = 1$ with an amplitude of $Q = 19\ \mu K$. The broken curve (corresponding to the right axis) shows the number of pairs of pixels contributing to the correlation function at each correlation function bin. For the analysis presented in the text, the correlation function is divided into 64 2.°8 bins, of which, only $n_c = 58$ contain data. Also, the correlation function at $\theta = 0$ (or, alternately, the *rms* of the data) is excluded from the analysis, as it is affected most by instrumental noise.

Fig. 2. — Likelihood contours for $R_{lim} = 430\ (\ \mu\mathrm{K})^2$, corresponding to a maximum of 171 simulations included within the test volume. The solid contours correspond to likelihoods of 0.05, 0.25, 0.5, and 0.75. The $\times$ at $(n, Q) \approx (1.0, 19\ \ \mu\mathrm{K})$ is the maximum and the broken lines correspond to likelihoods of 0.34 and 0.68. The inner broken line marks the $P(D|n,Q) = e^{-1/2}$ likelihood contour, while the outer broken line corresponds to $P(D|n,Q) = 0.34$. They are shown for comparison to other analyses. If one were to extract only the $n = 1$ portion of the plot, in the limit that the extracted likelihood is Gaussian, the $P(D|n,Q) = e^{-1/2}$ points would equal the 1σ credible limits assuming a uniform prior. The $P(D|n,Q) = 0.34$ contour represents the 68% credible limits if we use a prior of one for the models considered here and zero for all others. In other words, the sum of the likelihoods within the 0.34 contour is 68% of the sum of all the likelihoods in the figure.

Fig. 3. — Likelihood contours for various values of R_{lim}. The values of R_{lim} are 410, 420, 440 and 430 ($\mu\mathrm{K})^2$, moving clockwise from the top left. The maximum number of simulations within the test volumes for each case is indicated on the plots.

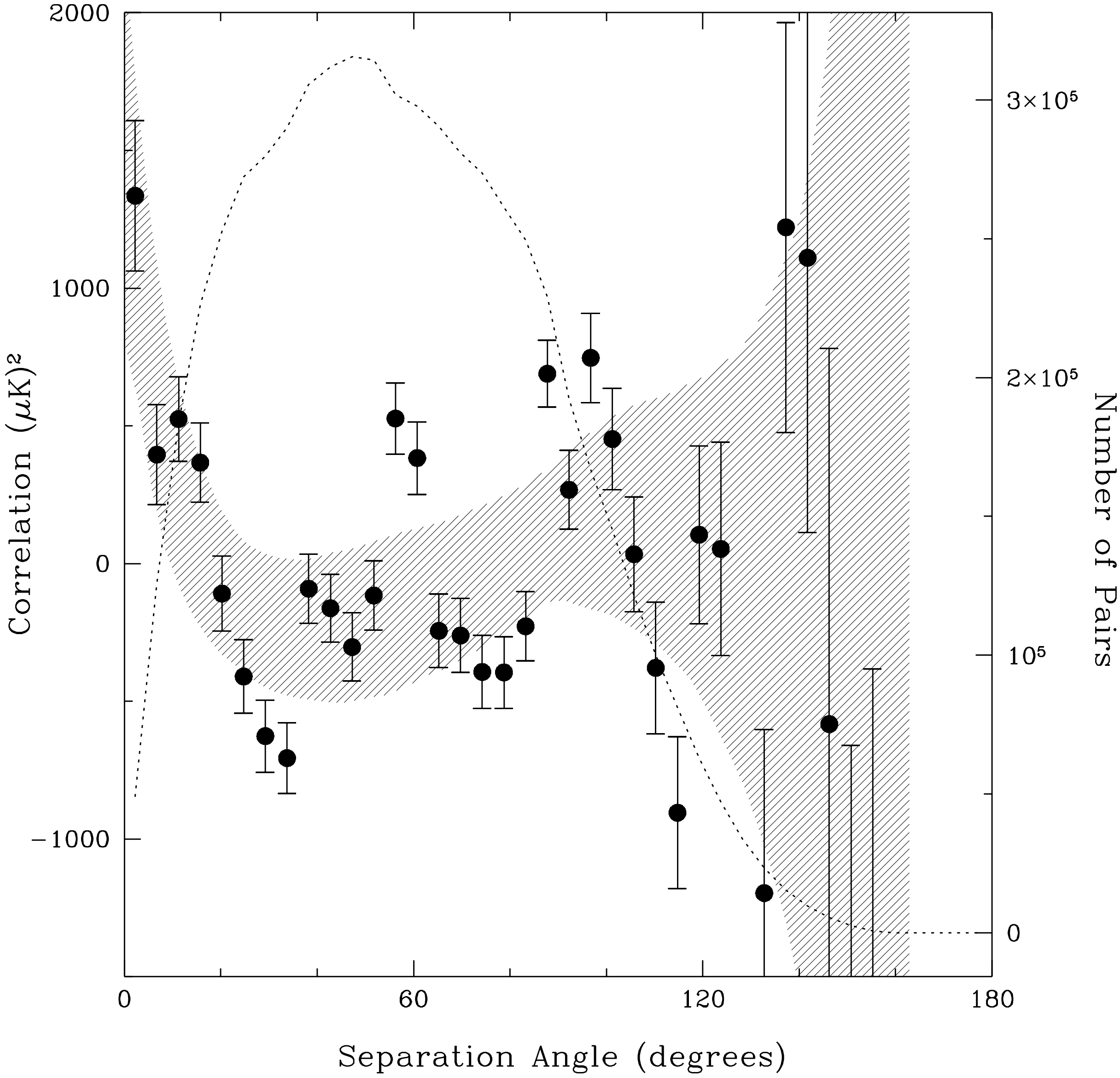
2000
1000
0
−1000
0
60
120
180
Separation Angle (degrees)
Correlation (μK)^2
Number of Pairs
3×10^5
2×10^5
10^5
0

Figure 1

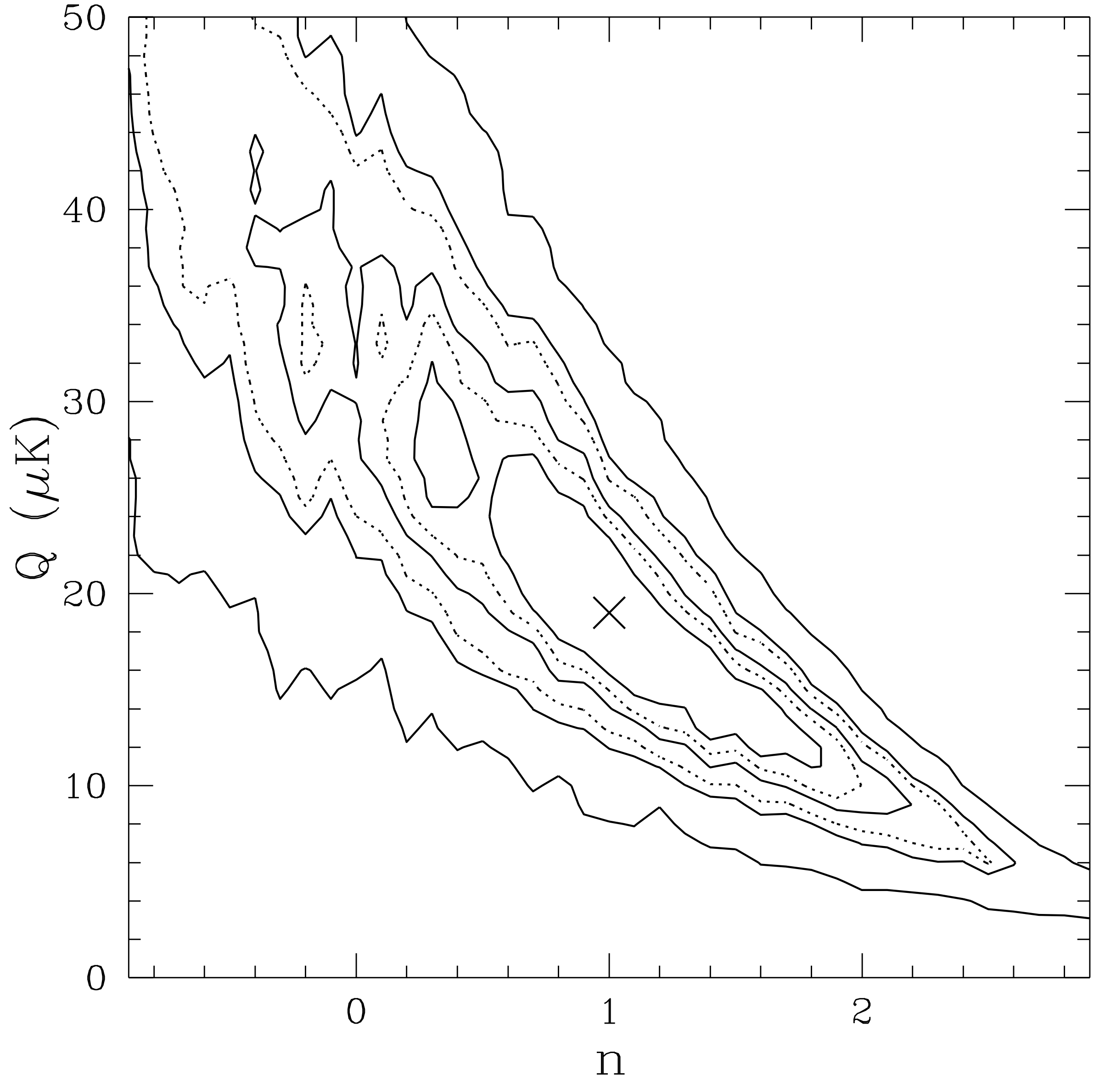

Figure 2

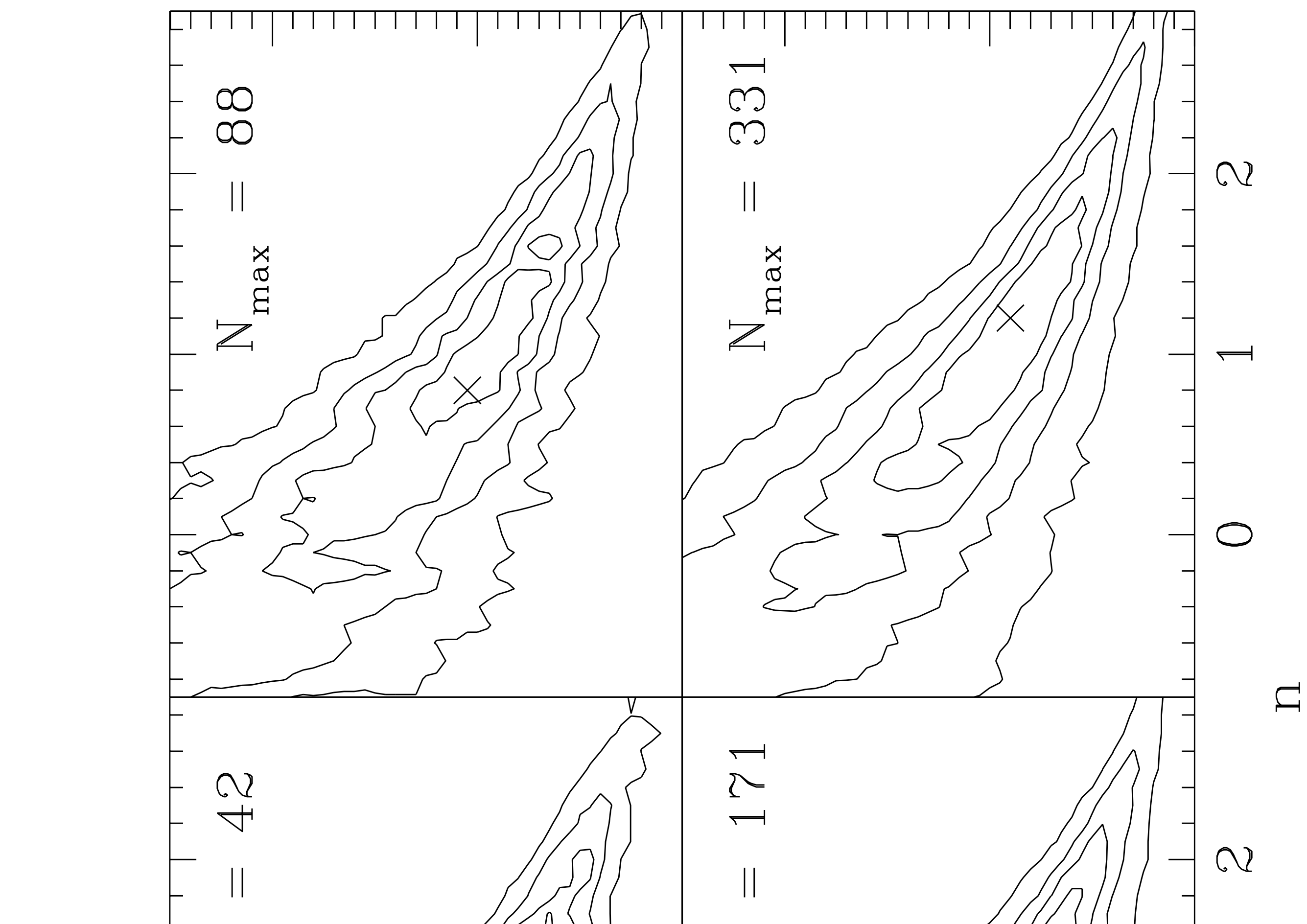

Figure 3